MASS-VELOCITY RELATION OF FRAGMENTS PRODUCED BY CATASTROPHIC IMPACTS; Yasuhiko Takagi and Manabu Kato, Department of Earth Sciences, Nagoya University, Chikusa-ku, Nagoya 464-01, Japan; Hitoshi Mizutani, Institute of Space and Astronautical Science, Yoshinodai 3–1–1, Sagamihara 229, Japan

Velocity distribution and energy partitionning of fragments produced by catastrophic collisions of planetesimals significantly affect the protoplanet growth. However, the experimental approach to this problem has not bee sufficient due to some technical difficulties. Only the velocity of a fragment splashed from the antipodal point (hereafter antipodal velocity) was scaled by a general scaling law using the nondimensional impact stress (NDIS) parameter (1, 2). As for the velocity distribution, recent experiments by Nakamura and Fujiwara (3) in a high velocity range determined three-dimensional velocities of some tens of fragments. Their results show that the fragment velocities are proportional to $m^{-1/6}$, suggesting that the kinetic energy is proportional to the surface energy. In this paper we report some results of our new series of impact experiments on three-dimensional velocities of fragments.

Experiments were performed in the impact velocity range of 140 to 650 m/sec. Targets were basalt and pyrophyllite. Projectiles were aluminum. Motions of fragments were recorded by a high-speed camera with a stereographic device in 1500–3000 frame/sec. The initial position and tree-dimensional velocity of each fragment was determined from the analysis of the films. Each recovered fragment was weighed and identified with the image on the film. The total mass of fragments of which velocities could be determined is 75 to 98 percent of the initial target mass.

Results shown in Fig. 1 are on the mass-velocity relation. In this figure, fragment velocities are normalized by the characteristic velocity (2), $v^* = Y/C_0\,\rho$, where Y, C_0, and ρ are the strength, bulk sound velocity, and density of the target, respectively. Fragment masses are also normalized by the original target mass, M_t. These results show that the velocity range of fragments except fine particles in the jetting is lather narrow, at most within a factor of 3. The present results also show that the mass dependence of velocity suggested by Nakamura and Fujiwara (3) is not evident.

Figure 2 shows the average (weighted by the mass) fragment velocity normalized by v^* and suggest that the v/v^*- NDIS relation is an appropriate scaling law to describe the overall fragment velocity as well as the antipodal velocity. On the other hand, this result shows that the energy partition to kinetic energy of basalt fragments is an order of magnitude larger than that of pyrophyllite fragments, because the normalizing velocity, v^*, of basalt is four times larger than that of pyrophyllite.

These results suggest the fragment velocity is not simply controlled by the surface energy, but by the shock wave strength and target properties which may yield complicated consequence of the shock wave generation,

expansion, and decay (2). Anyway, further experiments and analyses are necessary to complete understanding. The present method using the stereographic device will be a useful and powerful one for this purpose.

REFERENCES: (1) Takagi, Y., H. Mizutani, and S. Kawakami (1984) *Icarus*, **59**, 462–477; (2) Mizutani, H., Y. Takagi, and S. Kawakami (1990) *Icarus*, **87**, 307–326; (3) Nakamura, A. and A. Fujiwara (1990) Velocity distribution of fragments formed in simulated collisional disruption, submitted to *Icarus*

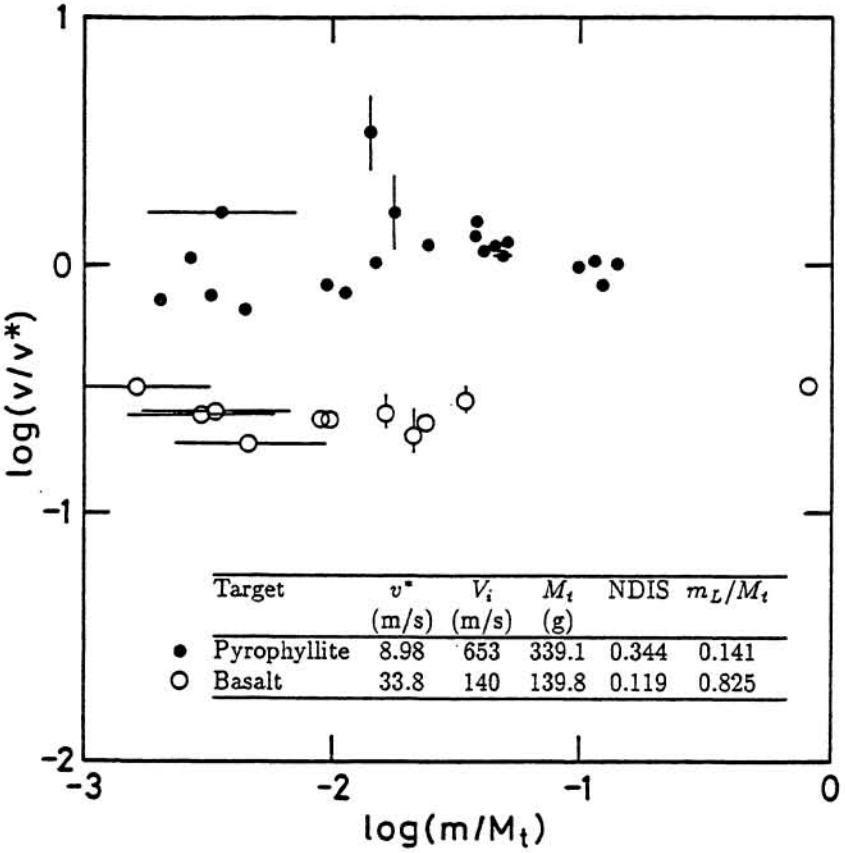

Fig. 1. Mass-velocity relations of fragments. Circles with horizontal errorbar show the data on images which were not identified with recovered fragments. The masses of these fragments were estimated from the projected areas on the film.

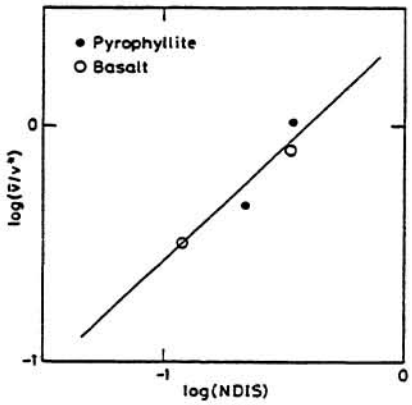

Fig. 2. Average fragment velocity normalized by v^* as a function of the nondimensional impact stress. The solid line is the antipodal velocity of the previous study (2).

MINERALOGICAL STUDIES OF LUNAR MARE METEORITES EET87521 AND Y793274; Hiroshi Takeda, Hiroshi Mori, Mineralogical Institute, Faculty of Science, Univ. of Tokyo, Hongo, Tokyo 113, Masamichi Miyamoto, College of Arts and Sci., Univ. of Tokyo, Komaba, Meguro-ku, Tokyo 153, Japan.

A new lunar meteorite EET87521 derived from a mare region of the Earth's Moon (1,2) has been studied by various mineralogical techniques and was compared with Y793274 with a similar origin (3). Clast types and pyroxene mineralogy have been used to identify the relationship to known lunar mare basalts. We investigated a polished thin section (PTS) EET87521,55 supplied by the Antarctic Meteorite Working Group (AMWG) by electron microprobe and scanning electron microscope (SEM) JEOL 840A and glassy matrices in small chips of Y793274 from NIPR (4) with an Hitachi H600 analytical transmission electron microscope (TEM) and JEOL 100CX TEM to see shock microtextures.

The EET87521,55 PTS consists of basaltic clasts and fragments of pyroxene, olivine, and plagioclase set in matrices of glassy materials. At one corner of the PTS, there is a large basaltic clast (BS1) 5.8 X 5.5 mm in size. Many parts of it are shock-disturbed and its subangular fragments are set in a brown swirly glass. The rounded laths of plagioclase are also shocked, and parts of them are maskelinitized or melted. The pyroxene crystals are up to 1.4 X 1.0 mm in size and show extensive chemical zoning in the pyroxene quadrilateral towards the Hd (hedenbergite) corner (Fig. 1). The pyroxene-plagioclase ratio (vol.) is about 2:1. A mesostasis portion consists of fayalite (Fa_{90}), ilmenite, and a silica mineral. The An-content of plagioclase crystals range from 92 to 82. Pyroxenes in other basaltic clasts (e.g. BS2) and fragments in the matrix show a similar chemical trend to BS1.

Of two plagioclase-rich clasts about 1 mm in diameter, one contains pyroxenes close to the Hd corner, but another (NR2) contains one of the Mg-rich pyroxenes with the least chemical zoning with Mg#[100 X Mg/(Mg+Fe)] =54 to 46. Because their plagioclase crystals show chemical zoning, these clasts are not highland plutonic rocks. One of the characteristics of EET87521 is that there are many fayalite fragments (Fa_{92} to Fa_{96}) with high Ca contents, which are zoned from Ca#[100 X Ca/(Ca+Mg+Fe)]=0.9 to 1.5 mol %.

Y793274,91-2 is a fragmental breccia richer in angular mafic minerals than plagioclase. Clast-laden glassy breccia and small number of glass spherules and glassy fragments are also present. In one region, fragments of pyroxene and olivine are set in a white (transparent) maskelinitized plagioclase matrix rimmed, in part, by swirly glass. One gabbroic clast (GB2) 0.8 X 0.4 mm in size consists of a rounded olivine 0.2 mm across in plagioclase and pyroxene. Their modal abundances (oliv:pyx:plag) are about 1:3:3. The An contents range from 96 to 89. The pyroxene is one of the most Mg-rich among the Y793274 pyroxenes ($Ca_{11}Mg_{61}Fe_{28}$) and shows fine exsolution lamellae of augite (1.2 μm wide with 2.3 μm interval). The olivine crystal (Fa_{35}) still preserves the initial zoning trend of CaO during crystal growth. Therefore, GB2 is not a plutonic rock. No lithic clasts of apparent plutonic highland origin have been recognized in the PTS. Inverted pigeonite or pyroxenes with coarse exsolution lamellae have not been found.

The chemical trends of the Y793274 pyroxenes are thus a combination of the zoning trends of quickly cooled lavas, and exsolved pyroxenes of different Mg# with limited Mg# range within one crystal. The most Mg-rich trend is the exsolution trend, whereas the Fe-rich trend is similar to those

of EET87521. The results suggest that the chemical variation is not due to the presence of many pyroxene-types from different crustal rocks as other lunar meteorites exhibited (5). The zoned pyroxene chemical trends of EET87521 and Y793274 may represent pyroxenes such as those reported for rare mare rock clasts found in Apollo 16 breccias and Luna 16 (6), and lunar meteorites (7). The original rock is coarse-grained. The Apollo 16 zoning trends cover more Mg-rich side of the pyroxene quadrilateral than EET87521. The most Fe-rich trend of EET87521 goes to that of hedenbergite in the HPF clast in Y791197 (8). The presence of such Fe-rich mineral fragments in EET87521 and Mg-rich clast such as GB2 in Y793274 suggest that these breccias represent thick lava flows of differentiated materials, and that the lavas originate close to the lunar highland from where many lunar meteorites were derived.

The microscopic features of matrices of EET87521 and Y793274 are similar. The TEM observation of Y793274 revealed that it is characterized by shock-produced melts of plagioclase, olivine and clinopyroxenes, etc. In plagioclase, shock-produced glass lamellae are often observed. The olivine crystal shows numerous dislocations, and no recovery was observed. The facts suggest that this sample has never reheated after the shock event.

In summary, EET87521 and Y793274 are fragmental breccias with minor regolith components and are rich in pyroxenes suggestive of mare origin (or non-crustal). The mare components are a coarse-grained rock similar to those with chemically zoned pyroxenes found in Apollo 16 breccias (eg. 60019,Ba-2) (6) and the VLT basalts in other lunar meteorites (7).

We thank AMWG and NIPR for the samples.

References:

(1) Warren, P. H. and Kallemeyn, G. W. (1989) Geochim. Cosmochim. Acta, 53, 3323-3300.
(2) Delaney J. S. (1989) Nature 342, 889-890.
(3) Takeda H., Saito J., Mori H., Yanai K., and Kojima H. (1990) Abstr. 15th Symp. Antarctic Meteorites 110-112, Natl. Inst. Polar Res., Tokyo.
(4) Yanai K., Kojima H. (compiled) (1987) Photographic Catalog of the Antarctic Meteorites, p. 216, NIPR, Tokyo.
(5) Takeda H., Miyamoto M., Mori H., Wentworth S. J. and McKay D. S. (1990) Proc. Lunar and Planet. Sci. Conf. 20th, 91-100.
(6) Takeda H., Miyamoto M., Galindo C. and Ishii T. (1987) Proc. Lunar Planet. Sci. Conf. 7th, J.G.R. 92, E462-E470.
(7) Treiman A. H. and Drake M. J. (1983) Geophys. Res. Lett. 10, 783-786.
(8) Takeda H., Mori H. and Tagai T. (1986) Mem. Natl Inst. Polar Res. Spec. Issue 41, 45-57.

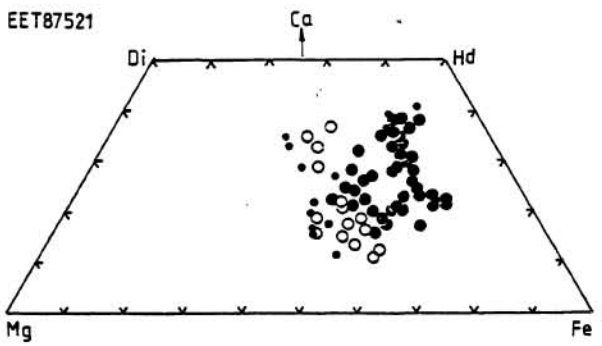

Fig. 1. Pyroxene quadrilateral of EET87521,55. Solid circles: BS1, dots: individual measurements, open circles: NR2.